

LI, Y., REN, J., YAN, Y., LIU, Q., PETROVSKI, A. and MCCALL, J. 2022. Unsupervised change detection in hyperspectral images using principal components space data clustering. *Journal of physics: conference series* [online], 2278: proceedings of the 6th International conference on machine vision and information technology (CMVIT 2022), 25 February 2022, [virtual event], article number 012021. Available from: <https://doi.org/10.1088/1742-6596/2278/1/012021>

# Unsupervised change detection in hyperspectral images using principal components space data clustering.

LI, Y., REN, J., YAN, Y., LIU, Q., PETROVSKI, A. and MCCALL, J.

2022

*Published under licence by IOP Publishing Ltd. Content from this work may be used under the terms of the Creative Commons Attribution 3.0 licence.*

PAPER • OPEN ACCESS

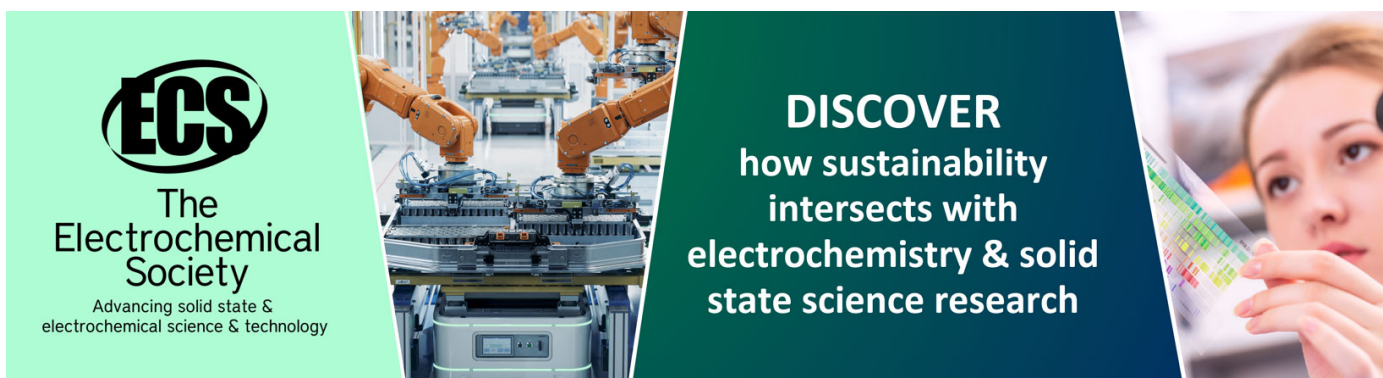
## Unsupervised Change Detection in Hyperspectral Images using Principal Components Space Data Clustering

To cite this article: Yinhe Li *et al* 2022 *J. Phys.: Conf. Ser.* **2278** 012021

View the [article online](#) for updates and enhancements.

You may also like

- [INVERSE PROBLEMS NEWSLETTER](#)
- [Special issue on applied neurodynamics: from neural dynamics to neural engineering](#)  
Hillel J Chiel and Peter J Thomas
- [Adiabatic representation for the three-body problem in hyperspherical coordinates. I. Statement of the problem](#)  
M B Kadomtsev and S I Vinitkii



**ECS**  
The  
Electrochemical  
Society  
Advancing solid state &  
electrochemical science & technology

**DISCOVER**  
how sustainability  
intersects with  
electrochemistry & solid  
state science research

# Unsupervised Change Detection in Hyperspectral Images using Principal Components Space Data Clustering

Yinhe Li<sup>1, a</sup>, Jinchang Ren<sup>1, b, \*</sup>, Yijun Yan<sup>1, c</sup>, Qiaoyuan Liu<sup>2, d</sup>, Andrei Petrovski<sup>1, e</sup> and John McCall<sup>1, f</sup>

<sup>1</sup> National Subsea Centre, Robert Gordon University, Aberdeen, AB21 0BH, U.K.

<sup>2</sup> Changchun Institute of Optics, Fine Mechanics and Physics, Chinese Academy of Sciences, Changchun, China

Corresponding Author: Prof. J Ren (<sup>b, \*</sup>j.ren@rgu.ac.uk); <sup>a</sup>y.li24@rgu.ac.uk; <sup>c</sup>y.yan2@rgu.ac.uk; <sup>d</sup>liuqy@ciomp.ac.cn; <sup>e</sup>a.petrovski@rgu.ac.uk; <sup>f</sup>j.mccall@rgu.ac.uk

**Abstract.** Change detection of hyperspectral images is a very important subject in the field of remote sensing application. Due to the large number of bands and the high correlation between adjacent bands in the hyperspectral image cube, information redundancy is a big problem, which increases the computational complexity and brings negative factor to detection performance. To address this problem, the principal component analysis (PCA) has been widely used for dimension reduction. It has the capability of projecting the original multi-dimensional hyperspectral data into new eigenvector space which allows it to extract light but representative information. The difference image of the PCA components is obtained by subtracting the two dimensionality-reduced images, on which the change detection is considered as a binary classification problem. The first several principal components of each pixel are taken as a feature vector for data classification using  $k$ -means clustering with  $k=2$ , where the two classes are changed pixels and unchanged pixels, respectively. The centroids of two clusters are determined by iteratively finding the minimum Euclidean distance between pixel's eigenvectors. Experiments on two publicly available datasets have been carried out and evaluated by overall accuracy. The results have validated the efficacy and efficiency of the proposed approach.

## 1. Introduction

With the development of remote sensing technology, hyperspectral imaging (HSI) can provide spatial and spectral information simultaneously in an image cube. Based on the ordinary 2-D spatial image, one additional spectral dimension is added, and the spectral data of each pixel is expanded to correspond to a spectral curve. HSI remote sensing has been widely used in many fields, such as geological exploration, geological mapping, environmental monitoring, and marine remote sensing et al. HSI data has the following characteristics [1]:

The spectrum has a wide band range and high spectral resolution: The spectral range obtained by the spectrometer can be extended from visible light to short infrared wave, and the spectral resolution can reach 10 *nm*. The number of bands of the image cube is up to hundreds, and the response of pixels forms a continuous spectral curve under different bands.



Detection and identification ability of surface coverage is greatly improved: HSI data can detect substances with diagnostic spectral absorption characteristics, and can accurately distinguish the types of surface vegetation cover and ground materials, etc.

There are also many challenges in processing hyperspectral image data. Different from multispectral images, hyperspectral images are composed of a large number of bands, and the correlation between adjacent bands is very high, resulting in information redundancy. Due to the problem of pixel mixing, the traditional image processing methods cannot be applied to hyperspectral image data processing. How to process hyperspectral image data efficiently and accurately is a challenge to be solved.

Change detection (CD) in remote sensing uses multi-temporal remote sensing data, uses a variety of image processing and pattern recognition methods to extract change information, quantitatively analyses and determines the characteristics and process of target change at different times [2]. Change detection is also one of the hotspots in the research of remote sensing application methods. The basic process of hyperspectral image change detection can be divided into three steps [3]: 1) Image pre-processing 2) Generate difference map 3) Analysis and evaluation difference diagram. The purpose of pre-processing is to make the multi-temporal image completely consistent in the spatial domain and spectral domain. The image is registered at the scale level or grey level through the scale invariant feature or mutual information feature in the spatial domain [4]. The errors caused by irradiation conditions and atmospheric radiation need to be corrected in the spectrum domain [5]. After image pre-processing, the key step is to extract and segment the change features in the difference image.

Based on the analysis of the algorithm, traditional hyperspectral image change detection can be divided into three categories. The first is based on Algebraic Operation, including change vector analysis (CVA), image difference, image ratio and so on [6]. This kind of method compares pixel by pixel and determines whether each pixel is changing through threshold setting. The advantage of this kind of method is that it can directly determine the change position without classifying the features first, which improves the detection efficiency. The disadvantage is that the result of change detection completely depends on the accuracy of radiometric correction and geometric correction.

The second category is based on Image Transformation, such as independent component analysis (ICA), principal component analysis (PCA), multivariate alteration detection (MAD) and so on. The principle of these methods is to project or compress the original hyperspectral image data into a new feature space and mark the changed pixels. This kind of method can make full use of the spectral domain information, but it will destroy the similarity of adjacent pixels and the continuity of adjacent bands in the new feature space [7].

The third category is for all other algorithms, such as unmixing-based, classification-based, deep-learning method and so on [8]-[9]. This kind of change detection methods are based on statistical features, texture features or spatial structure algorithm.

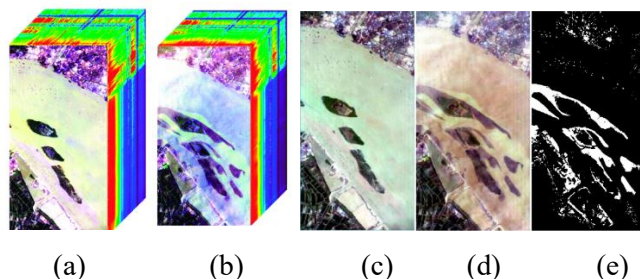


**Figure 1:** Illustration of the Experiment dataset (a) River scene on May 3, 2013 (b) River scene on December 31, 2013. (c) Pseudo-color image at  $T_1$  (d) Pseudo-color image at  $T_2$  (e) Ground truth change map

Figure 1 shows two hyperspectral datasets for change detection, which were collected from a river area in Jiangsu Province, China on May 3 and December 31, 2013. The spectrometer carried on the satellite is earth Observing-1 (EO-1) Hyperion, with a spectral range of  $0.4\text{-}2.5\mu\text{m}$ . The spectral resolution is  $10\text{ nm}$  and the spatial resolution is  $30\text{ m}$ . The size of this HSI dataset after geometric correction and atmospheric correction is  $463 * 241$  pixels and has 198 spectral bands respectively [10].

## 2. Methodology

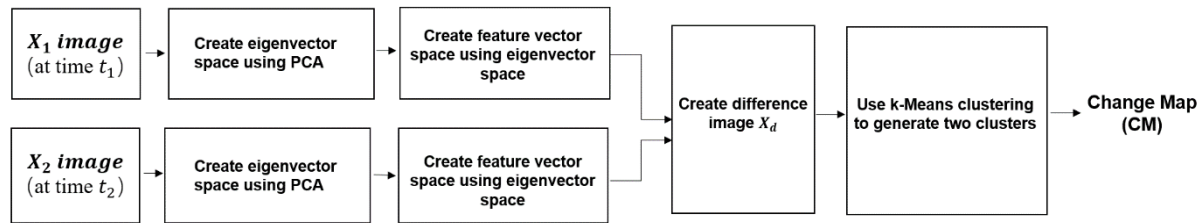


**Figure 2:** General scheme of the proposed PCA based K-Means approach

Figure 2 shows the general scheme of PCA based on K-means approach. This approach was first proposed by Turgay Celik in 2009. The first step is to reduce two input HSI images to the same specified dimension  $k$  by using PCA, create eigenvector space for  $X_1$  and  $X_2$  respectively. Then create feature vector using eigenvector space. Next, the difference image  $X_d$  is obtained by subtracting the two dimensionally reduced images. Finally, the feature vector in  $X_d$  was divided into two clusters by K-means clustering. The minimum Euclidean distance is used to calculate the distance between each pixel and the centroid of two clusters, all pixels are assigned to two clusters to obtain the change map.

PCA is a traditional feature extraction algorithm, which aims to find the orthogonal projection space with the largest variance. When projected into the new space, the correlation between features will be eliminated, and all information will be concentrated in a few top bands, to realize information extraction and dimensionality reduction. Perform PCA processing on the two images separately, which can effectively retain the feature information of the original image. Assume two HSI cubes  $X_1$  and  $X_2$  have  $p$  continuous bands at  $t_1$  and  $t_2$  respectively. The covariance matrix of  $X_1$  is given by:

$$\Sigma_1 = \frac{1}{n-1} X_1 X_1^T \quad (1)$$

The projection matrix of PCA is mainly calculated by the following eigenvalue decomposition:

$$\Sigma_1 W_1 = \Lambda_1 W_1 \quad (2)$$

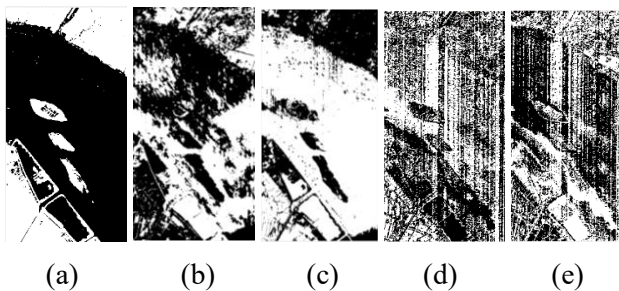
$\Sigma_1$  is Image covariance matrix,  $W_1$  is the corresponding eigenvector matrix,  $\Lambda_1$  is the diagonal matrix of eigenvalues, arranged from large to small according to eigenvalues. Select the largest  $K$  of eigenvalues as principal component. Then, the corresponding  $K$  eigenvectors are used as row vectors to form the eigenvector matrix  $P_1$ .

Convert the matrix  $P_1$  into the new space constructed by  $K$  eigenvectors, can obtain the objection matrix in eigenvector space which reduced to  $K$  dimension, that is:

$$Y_1 = P_1 X_1 \quad (3)$$

Similarly, by extracting the largest  $K$  eigenvalues and eigenvectors of  $X_2$ , created the reduced-dimensional objection matrix in eigenvector space:

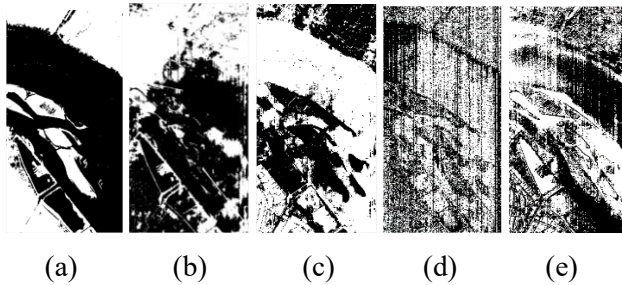
$$Y_2 = P_2 X_2 \quad (4)$$



**Figure 3:** Top 5 principal components of image  $T_1$ : (a) First PC, (b) Second PC, (c) Third PC, (d) Fourth PC, (e) Fifth PC

**Table 1:** Cumulative proportion of Top five principal components

	PC1	PC2	PC3	PC4	PC5
$T_1$	0.9190	0.9679	0.9895	0.9924	0.9946
$T_2$	0.9212	0.9647	0.9842	0.9895	0.9914

**Figure 4:** Top 5 principal components of image  $T_2$ : (a) First PC, (b) Second PC, (c) Third PC, (d) Fourth PC, (e) Fifth PC

PCA dimensionality reduction is performed on two input HSI cubes  $X_1$  and  $X_2$  respectively. The reason for taking the top five principal components is to extract the least eigenvalues on the basis of retaining the largest original information and ensure both input images can retain at least 99% feature information. After PCA dimensionality reduction, 99.46% of the components can be retained for image  $T_1$  and 99.14% for  $T_2$ . The first five Principal components' grayscale images on each dimension were shown in figures 3 and figure 4. And the cumulative proportion of the first five PCs were recorded in Table 1. The difference image  $X_d$  is obtained by absolute-valued intensity values of these two input image cubes. Next, use K-Means clustering method to segment  $X_d$  to obtain the change map.

$$X_d = |Y_2 - Y_1| \quad (5)$$

Clustering is an unsupervised learning method, which divides the data into different classes or clusters through iteration, so that the similarity between the data in the same cluster and the difference between different clusters are as large as possible [11]. Clustering algorithm is a common method in the change information segmentation step of hyperspectral remote sensing image change detection. The common clustering method is K-means clustering.

Assume a sample set containing  $m$  samples in  $X_d = \{\vec{x}_1, \vec{x}_2, \dots, \vec{x}_m\}$ , two clusters can be obtained by K-means clustering  $C = \{C_1, C_2\}$ . The centroid of cluster  $C_i$  is  $\mu_i = \frac{1}{c} \sum \vec{x}$ . The pixels in the first cluster represent the changes region in the difference image  $X_d$ , the other cluster represents the non-changed region [12]. The goal of K-means clustering is to find the minimum square difference between the eigenvectors and the centroid through Euclidean distance iteration.

$$E = \sum_{i=1}^k \sum_{\vec{x} \in C_i} \|\vec{x} - \mu_i\|_2^2 \quad (6)$$

### 3. Experiment Results

#### 3.1 Algorithm Evaluation

The pixels in the difference image are binary clustered. The changed pixel is replaced by 1 and the unchanged pixel is replaced by 0 to generate a binary change map  $\Omega$ .

$$\Omega(i, j) = \begin{cases} 1 & \text{Changed pixels (Cluster 1)} \\ 0 & \text{Non-changed pixels (Cluster 2)} \end{cases} \quad (7)$$

By comparing  $\Omega$  with the reference image GT, we can calculate the overall accuracy as follows, where  $N_c$  and  $N$  denote respectively the number of the matched pixels and the overall image pixels:

$$ACC = \frac{N_c}{N} \tag{8}$$

3.2 Results comparison

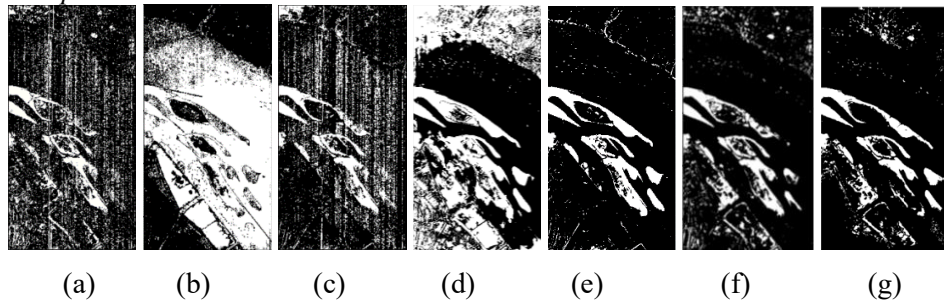


**Figure 5:** Change map results of river dataset: (a) Difference, (b) Ratio, (c) CVA, (d)PCA based OTSU, (e) K-Means, (f) PCA based K-Means, (g) Ground truth

OTSU algorithm divides pixels in difference image into background and foreground, the changed pixels are the foreground, and the unchanged pixels are the background, calculated the threshold when the variance between background and foreground is the largest [13]. Five comparison different feature extraction algorithms were used to get the difference matrix, and then use OTSU threshold segmentation method to get the final change map. Binary change map results of all algorithms were shown in Figure 5. The purpose of experiments (d) and (f) were tested the comparison overall accuracy results of these two threshold segmentation methods: OTSU and K-Means. Experiments (e) and (f) were compared the overall accuracy results by using PCA based K-Means with the method of using K-Means directly on the original difference image. The overall accuracy results of all algorithms used in experiment 1 were listed in Table 2.

**Table 2:** Overall accuracy of experiment 1

	Difference	CVA	Ratio	PCA OTSU	K-Means	PCA K-Means
<b>Overall Accuracy</b>	0.8027	0.7115	0.5679	0.8240	0.9209	0.9419

Compared with three conventional algorithms: Difference, CVA and Ratio. The algorithm based on PCA gave a good performance is this experiment. The overall accuracy of PCA based on OTSU and k-means algorithms can reach 82.10% and 94.19% respectively. The overall accuracy obtained by using the K-Means clustering algorithm directly on the original difference image in experiment (e) is 92.09%. The overall accuracy of change detection algorithm based PCA is much higher than the other algorithms. This is because when extracting the PCs of the input image, the correlation between each band of the HSI was destroyed, the invalid band and features were eliminated in difference image and the characteristics of the original information were well preserved.

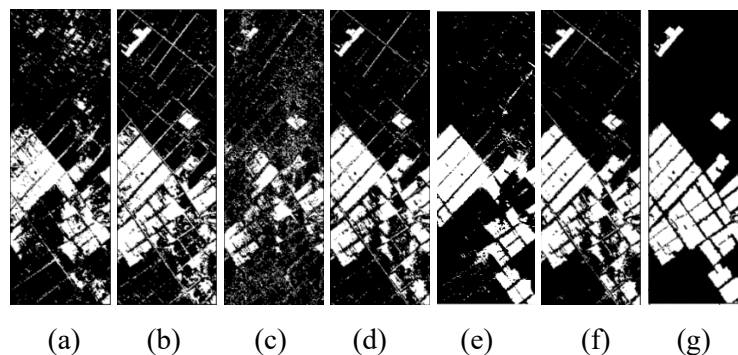


**Figure 6:** Change map results of the Yancheng dataset: (a) Difference, (b) Ratio, (c) CVA, (d)PCA based OTSU, (e) K-Means, (f) PCA based K-Means, (g) Ground truth

**Table 3:** Overall accuracy of Experiment 2

	Difference	CVA	Ratio	PCA OTSU	K-Means	PCA K-Means
<b>Overall Accuracy</b>	0.8127	0.7962	0.7331	0.8608	0.8203	0.8785

The validation experiment was carried out on the China farmland dataset. The bitemporal images were collected in Yancheng City, Jiangsu Province, China on May 3, 2006 and April 23, 2007, respectively [14]. The HSI cube consists of 420 \* 140 pixels and 154 bands. Binary change map results of all algorithms used in experiment were shown in Figure 6. The change detection algorithm of PCA based K-means still has good detection effect compared with other conventional algorithms, the overall accuracy is 87.85%, outperforming all others as shown in Table 3.

#### 4. Conclusion

In this paper, introduced the change detection algorithm of hyperspectral image using Principal components analysis based on K-Means. PCA can well reduce the dimension of the original image cube and retain the effective features. K-means clustering calculates the minimum Euclidean distance of all pixels by iterative method and divides the feature information into changed region and non-changed region. Compared experimental results on two publicly available datasets to demonstrated that PCA based K-Means HSI change detection algorithm had the best detection performance than other conventional methods, which giving higher overall accuracy.

#### References

- [1] Yan Y, et al.. Nondestructive Phenolic Compounds Measurement and Origin Discrimination of Peated Barley Malt Using Near-Infrared Hyperspectral Imagery and Machine Learning. *IEEE Trans. on Instrumentation and Measurement*. 2021 May 21; 70:1-5.
- [2] Wu C, Du B, Zhang LP. Hyperspectral change detection based on independent component analysis. *Yaogan Xuebao- Journal of Remote Sensing*. 2012 May;16(3):545-61.
- [3] Bioucas-Dias JM, et al. Hyperspectral remote sensing data analysis and future challenges. *IEEE Geoscience and remote sensing magazine*. 2013 Jul 9;1(2):6-36.
- [4] Gong M, et al. A novel coarse-to-fine scheme for automatic image registration based on SIFT and mutual information. *IEEE Trans. on Geoscience and Remote Sensing*. 2013 Oct 3;52(7):4328-38.
- [5] Liu SC, et al. Statistical change detection with moments under time-varying illumination. *IEEE Trans. on Image Processing*. 1998 Sep;7(9):1258-68.
- [6] Kwan C. Methods and challenges using multispectral and Hyperspectral images for practical change detection applications. *Information*. 2019 Nov;10(11):353.
- [7] Zhang B, et al. Real-time target detection in hyperspectral images based on spatial-spectral information extraction. *EURASIP journal on advances in signal processing*. 2012 Dec;2012(1):1-5.
- [8] Liu S, et al. Unsupervised multitemporal spectral unmixing for detecting multiple changes in hyperspectral images. *IEEE Trans. on Geoscience and Remote Sensing*. 2016 Jan 12;54(5):2733-48.
- [9] Wang Q, et al. GETNET: A general end-to-end 2-D CNN framework for hyperspectral image change detection. *IEEE Trans. on Geoscience and Remote Sensing*. 2018 Jul 24;57(1):3-13.
- [10] Song A, et al. Change detection in hyperspectral images using recurrent 3D fully convolutional networks. *Remote Sensing*. 2018 Nov;10(11):1827.
- [11] Celik T. Unsupervised change detection in satellite images using principal component analysis and k-means clustering. *IEEE Geoscience and Remote Sensing Letters*. 2009 Aug 7;6(4):772-6.



- [12] Ghosh S, Mishra NS, Ghosh A. Unsupervised change detection of remotely sensed images using fuzzy clustering. *In 2009 7<sup>th</sup> Int. Conf. on Advances in Pattern Recognition* 2009 Feb 4 (pp. 385-388). IEEE.
- [13] Otsu N 1975 A threshold selection method from gray-level histograms, *Automatica* 11, 23–27
- [14] Hanley JA, McNeil BJ. The meaning and use of the area under a receiver operating characteristic (ROC) curve. *Radiology*. 1982 Apr;143(1):29-36.